Melanin-concentrating hormone 1 receptor-deficient mice are lean, hyperactive, and hyperphagic and have altered metabolism

Donald J. Marsh*[†], Drew T. Weingarth*, Dawn E. Novi*, Howard Y. Chen*, Myrna E. Trumbauer*, Airu S. Chen*, Xiao-Ming Guan*, Michael M. Jiang*, Yue Feng*, Ramon E. Camacho‡, Zhu Shen*, Easter G. Frazier*, Hong Yu*, Joseph M. Metzger‡, Stephanie J. Kuca‡, Lauren P. Shearman‡, Shobhna Gopal-Truter§, Douglas J. MacNeil*, Alison M. Strack‡, D. Euan MacIntyre‡, Lex H. T. Van der Ploeg*, and Su Qian*[†]

Departments of *Obesity Research, ‡Animal Pharmacology, and §Comparative Medicine, Merck Research Laboratories, Rahway, NJ 07065

Melanin-concentrating hormone (MCH) is a cyclic 19-aa hypothalamic neuropeptide derived from a larger prohormone precursor of MCH (Pmch), which also encodes neuropeptide EI (NEI) and neuropeptide GE (NGE). Pmch-deficient (Pmch−/−) mice are lean, hypophagic, and have an increased metabolic rate. Transgenic mice overexpressing Pmch are hyperphagic and develop mild obesity. Consequently, MCH has been implicated in the regulation of energy homeostasis. The MCH 1 receptor (MCH1R) is one of two recently identified G protein-coupled receptors believed to be responsible for the actions of MCH. We evaluated the physiological role of MCH1R by generating MCH1R-deficient (Mch1r−/−) mice. Mch1r−/− mice have normal body weights, yet are lean and have reduced fat mass. Surprisingly, Mch1r−/− mice are hyperphagic when maintained on regular chow, and their leanness is a consequence of hyperactivity and altered metabolism. Consistent with the hyperactivity, Mch1r−/− mice are less susceptible to diet-induced obesity. Importantly, chronic central infusions of MCH induce hyperphagia and mild obesity in wild-type mice, but not in Mch1r−/− mice. We conclude that MCH1R is a physiologically relevant MCH receptor in mice that plays a role in energy homeostasis through multiple actions on locomotor activity, metabolism, appetite, and neuroendocrine function.

M elanin-concentrating hormone (MCH) is expressed in the central nervous system predominantly in neurons in the lateral hypothalamus and zona incerta, which project broadly throughout the brain (1, 2). MCH mRNA levels are increased in response to fasting and are elevated in leptin-deficient *ob/ob* mice relative to control mice (3), suggesting that leptin negatively regulates MCH. Rodent pharmacology further supports a role for MCH in the control of energy homeostasis, as centrally administered MCH stimulates food intake in rats (3, 4).

In addition to MCH, prohormone precursor of MCH (Pmch) also encodes neuropeptide EI (NEI) and neuropeptide GE (NGE) (5) and may potentially give rise to an alternative splice variant termed MCH-gene-overprinted-polypeptide (MGOP; ref. 6), as well as encode a portion of the recently identified antisense-RNA-overlapping-MCH (AROM; ref. 7). Two recently described mouse genetic models further implicate MCH in the regulation of energy homeostasis. *Pmch−/−* mice are lean, hypophagic, and have an increased metabolic rate (8). In contrast, transgenic mice overexpressing *Pmch* develop mild obesity, are hyperphagic, and become insulin-resistant (9). As both these models represent genetic manipulations of *Pmch*, one must consider the possibility that in addition to alterations in MCH, changes in the levels of NEI and NGE, as well as potentially MGOP and AROM, may also contribute to the phenotypes of these models.

The MCH 1 receptor (MCH1R) was initially identified as an orphan G protein-coupled receptor that bound MCH with high affinity (10). Subsequently, a second high-affinity MCH receptor

(MCH2R) with moderate amino acid identity to MCH1R was identified in humans (11–15). Both receptors are highly selective for MCH and are not activated by NEI, neuropeptide GE, or MCH-gene-overprinted-polypeptide (13, 16, 17); however, *in vivo* validation for these receptors is still lacking. We generated *Mch1r−/−* mice to evaluate the physiological function of MCH1R, and to determine whether it is involved in mediating the effects of MCH on energy homeostasis. Additionally, we hoped to gain insight into what aspects of the *Pmch−/−* and *Pmch* overexpressing phenotypes are likely attributed to MCH.

Materials and Methods

Animal Care and Maintenance. All animal protocols used in these studies were approved by the Merck Research Laboratories Institutional Animal Care and Use Committee in Rahway, NJ. We housed mice in microisolator cages (Lab Products, Maywood, NJ) in a barrier facility with an air shower entrance or in a specific pathogen-free facility. Mice were maintained on either regular chow [Teklad (Madison, WI) 7012: 14.8% kcal from fat; Harlan Teklad], a moderate-fat diet (D12266B: 32% kcal from fat; Research Diets, New Brunswick, NJ), or a high-fat diet (Teklad 97070: 60% kcal from fat) with ad libitum access to water in a 12-h/12-h light/dark cycle unless stated otherwise.

Generation of *Mch1r−/−* Mice. We screened a mouse 129SvEv genomic library (Lambda FIX II vector, Stratagene) with a 500-bp mouse *Mch1r* cDNA probe, which was generated by PCR using primers derived from rat *SLC-1* sequences (18). One positive clone containing a 14-kb *Mch1r* genomic sequence was isolated. Two regions of the clone were subcloned into pBluescript vector (Stratagene). We generated an *Mch1r* targeting vector by inserting a 6.5-kb 5′ *Kpn*I to *Kpn*I restriction fragment into the *Kpn*I site and a 1.4-kb 3′ *Bam*HI to *Xba*I restriction fragment between *Cla*I and *Sac*II sites of pKO Scrambler 1901 (Stratagene). The targeting vector was linearized by *Not*I digestion and transformed into AB2.2 embryonic stem (ES) cells by electroporation with a Bio-Rad Gene Pulser. We cultured transfected cells with G418 and FIAU for positive and negative selections, respectively. Approximately 500 clones were selected, and 10 correctly targeted ES cell clones were identified by Southern blot analysis. We injected correctly targeted ES clones

---

into C57BL/6 blastocysts and then implanted these into pseudopregnant female mice (19). Several chimeric progeny gave germ-line transmission of the mutant *Mch1r* allele and two independent *Mch1r*$^{+/-}$ lines were established. F$_2$ hybrid mice were used in all experiments except the high-fat diet study, which involved F$_3$ hybrids.

Genotyping. We performed Southern blot analysis by using a 3′ probe and a coding region probe (20). The 3′ flanking probe is a 0.95-kb PCR fragment located 180 bp 3′ of the short arm of the targeting vector. After *Eco*RV and *Hpa*I digestion, this probe should detect a 6.0- and 4.2-kb band from the wild-type and mutant *Mch1r* alleles, respectively. The coding region probe is a 1.1-kb *Kpn*I to *Bam*HI restriction fragment of *Mch1r*, spanning the first transmembrane domain to the stop codon, which should detect a 6.0-kb wild-type band from *Eco*RV- and *Hpa*I-digested genomic DNA and should not detect a signal from the mutant allele.

***In Situ* Hybridization.** *In situ* hybridization was performed as described (21), using an equal molar mixture of two nonoverlapping antisense oligonucleotides directed against *Mch1r*. Oligonucleotide sequences are available on request.

Growth Curves. We housed littermate mice from several different litters two per cage and provided them with ad libitum access to regular chow and water. Within any given age group, there was an equal representation of each genotype. Body weights and food intake were measured weekly starting at 6 weeks of age.

Feeding Behavior. We separated mice into individual microisolator cages at least 7 days before measuring food intake. For studies involving regular mouse chow or the medium high-fat diet, we provided pellet food in wire cage tops containing food hoppers and weighed food daily. Food weights from 4–5 consecutive days were used to calculate daily food intake. For studies involving the high-fat diet, we provided ground food in a glass jar located in the cage and weighed the jar weekly. We measured the duration and frequency of feeding and drinking with an automated food intake system (Mini-Mitter, Sunriver, OR). For studies involving the automated food intake system, we provided ground regular chow in a food hopper attached to the side of the cage and weighed the food hopper daily.

Motor Activity. We evaluated ambulatory activity and fine movements of individually housed mice with a cage rack Photobeam Activity System (San Diego Instruments) as described (22).

Body Composition. We analyzed whole body composition by dual energy x-ray absorptiometry (DEXA; QDR 4500, Hologic, Waltham, MA), using the QDR 4500 SMALL ANIMAL STUDIES software version 9.0 as described (22).

Plasma Measurements. We measured plasma leptin, insulin, total T4, and corticosterone levels as described (22). Plasma glucose and triglyceride levels were measured by enzyme-colorimetric assays (Sigma and Roche Diagnostics, respectively).

Indirect Calorimetry. We measured metabolic rate by indirect calorimetry with a 16-chamber open-circuit Oxymax system (Columbus Instruments, Columbus, OH) as described (22).

Intracerebroventricular Cannulations and Injections. We anesthetized mice with an i.m. injection of ketamine (100 mg/kg) and domitor (0.75 mg/kg) and placed them in a sterotactic device (Kopf Instruments, Tujunga, CA). A 26-gauge single acute guide cannula (Plastics One, Roanoke, VA) was implanted into either the left lateral ventricle (0.22 mm posterior, 1.0 mm lateral, and 2.3 mm ventral to bregma) or the dorsal third ventricle (0.22 mm
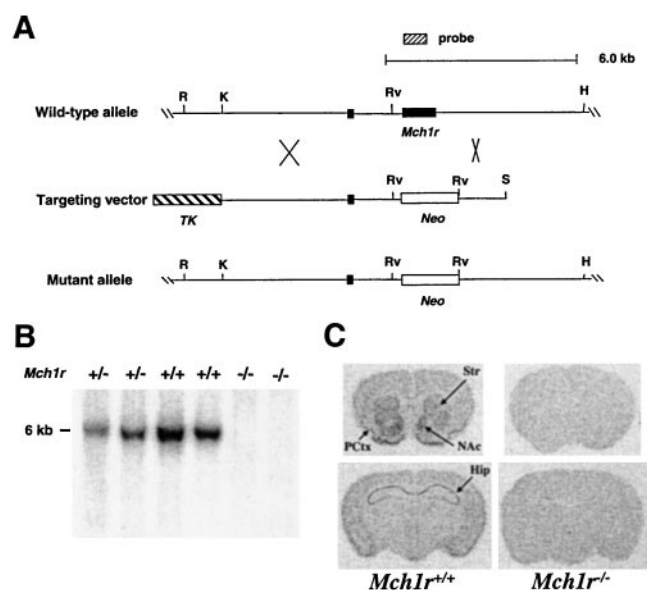

Fig. 1. Targeted disruption of *Mch1r*. (*A*) Illustrations and partial restriction map of the mouse *Mch1r* wild-type allele, targeting vector, and mutant allele. Filled, open, and hatched boxes represent exons, the neomycin-resistance cassette (*Neo*), and the probe used for Southern blot analysis in *B* or the thymidine kinase gene (*TK*), respectively. R, *Eco*RI; K, *Kpn*I; Rv, *Eco*RV; S, *Sal*I; H, *Hpa*I. (*B*) Southern blot analysis of tail DNA from wild-type (*Mch1r*$^{+/+}$), Mch1r$^{+/-}$, and *Mch1r*$^{-/-}$ mice using the *Mch1r* coding region probe depicted in *A*. Genomic DNA was digested with *Eco*RV and *Hpa*I. (*C*) *In situ* hybridization performed on coronal brain sections from *Mch1r*$^{+/+}$ and *Mch1r*$^{-/-}$ mice. NAc, nucleus accumbens; Hip, hippocampus; PCtx, piriform cortex; Str, striatum.

posterior, 0.3 mm lateral, and 3.3 mm ventral to bregma). After surgery, a 33-gauge dummy cannula (Plastics One) was inserted into each guide cannula and mice were given an i.m. injection of antisedan (5 mg/kg). All cannulated mice were given 1 week of postoperative recovery during which time they were handled daily to minimize nonspecific stress. All substances were administered to conscious mice with a repeating dispenser (Hamilton) equipped with a 50-μl Hamilton syringe and 33-gauge needle designed to extend 0.1–0.2 mm beyond the tip of the guide cannula. We dissolved neuropeptide Y (NPY), MCH (Peninsula Laboratories), and agouti-related protein (AgRP)83–132 amide (Phoenix Pharmaceuticals, St. Joseph, MO) in artificial cerebrospinal fluid (Harvard Apparatus) and injected all substances in a total volume of 2 μl. Mice were given at least a 48-h recovery period between treatments. All intracerebroventricular injection studies were of crossover design. We verified cannulae placement at the end of the experiment by injection of 2 μl of a 1% cresyl violet solution, removal of the brain, and examination of coronal brain slices. For chronic infusion studies, we used 28-gauge osmotic pump connector cannulae (Plastics One) connected by vinyl tubing to microosmotic pumps designed to deliver 0.5 μl/h (Alza).

Statistical Analysis. We reported all values as mean ± SEM and analyzed data by the two-tailed unpaired Student's *t* test or one-way ANOVA (factorial) when appropriate. *P* values ≤ 0.05 were reported as significant.

Results

Generation and Validation of *Mch1r*$^{-/-}$ Mice. *Mch1r* encodes a 355-aa protein with seven transmembrane domains. We replaced a 1.1-kb region of exon 2, extending from the first transmembrane domain to the stop codon, with a neomycin-resistance cassette (Fig. 1*A*). Two lines of *Mch1r*$^{+/-}$ mice were established
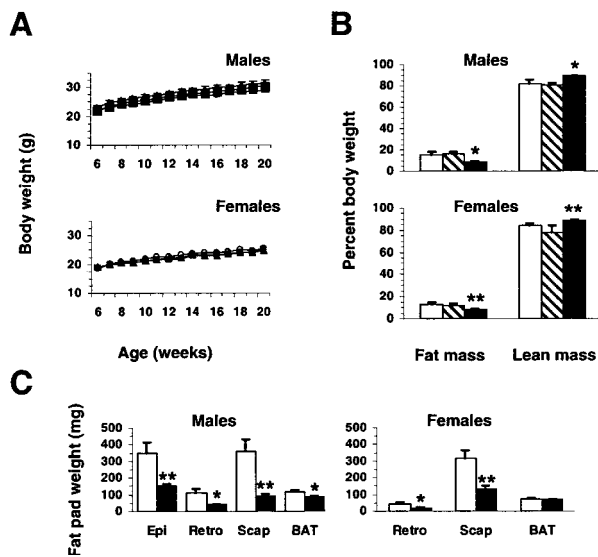
Fig. 2. Growth and body composition of control and Mch1r⁻/⁻ mice maintained on regular chow. (A) Growth curves of group-housed male and female wild-type (Mch1r⁺/⁺; filled squares), Mch1r⁺/⁻ (filled triangles), and Mch1r⁻/⁻ littermate mice (open circles; n = 14–16 per group). (B) DEXA analysis of 5–7-month-old group-housed male and female Mch1r⁺/⁺ (white bars), Mch1r⁺/⁻ (hatched bars), and Mch1r⁻/⁻ (shaded bars; n = 12–14 per group) littermates from A. (C) Adipose tissue mass in Mch1r⁺/⁺ (white bars) and Mch1r⁻/⁻ littermates (shaded bars; n = 14 per group) from B. Epi, epididymal; Retro, retroperitoneal; Scap, scapular white, BAT, interscapular brown. All P values are from comparisons between Mch1r⁺/⁺ and Mch1r⁻/⁻ littermates. **, $P < 0.01$; *, $P < 0.05$.

from independent embryonic stem cell clones. Mating of male and female Mch1r⁺/⁻ mice produced all three genotypes in the expected Mendelian ratio (Mch1r⁺/⁺ mice, 310; Mch1r⁺/⁻ mice, 662; Mch1r⁻/⁻ mice, 345). Southern blot analysis (Fig. 1B) and *in situ* hybridization (Fig. 1C) confirmed the absence of Mch1r in Mch1r⁻/⁻ mice.

Growth Curves and Body Composition. Mch1r⁻/⁻ mice of both genders were fertile and exhibited no gross histological or pathological abnormalities. Group-housed wild-type, Mch1r⁺/⁻, and Mch1r⁻/⁻ littermates of both genders and from both lines exhibited similar growth (Fig. 2A); however, DEXA revealed that both male and female 5–7-month-old Mch1r⁻/⁻ mice were significantly leaner than wild types (Fig. 2B). Both genders of Mch1r⁻/⁻ mice possessed ≈50% less fat mass and ≈7% more lean mass than wild types. Male and female Mch1r⁺/⁻ mice exhibited normal body composition. Evaluation of a subset of individual fat pads (Fig. 2C) and DEXA analysis of individually housed animals from the second line (data not shown) corroborated the lean phenotype.

Food Intake. Surprisingly, both individually housed (Fig. 3A) and group-housed (data not shown) Mch1r⁻/⁻ mice of both genders maintained on regular chow were significantly hyperphagic relative to littermate controls. Male and female Mch1r⁻/⁻ mice consumed 15.8% and 12.3%, respectively, more regular chow than controls. Hyperphagia in the range of 12–24% was consistently observed in several different cohorts of male and female Mch1r⁻/⁻ mice from both lines (data not shown). We measured daily feeding and drinking durations to define the hyperphagia further. The hyperphagia was a consequence of significantly increased feeding duration (Fig. 3B) and was associated with increased drinking duration (data not shown). Increases in both behaviors were restricted entirely to the dark phase of the
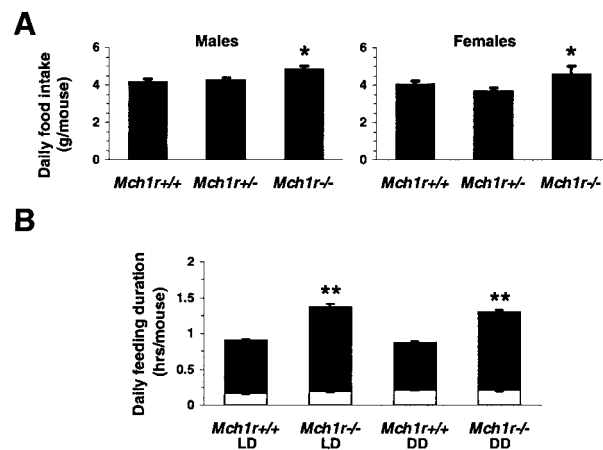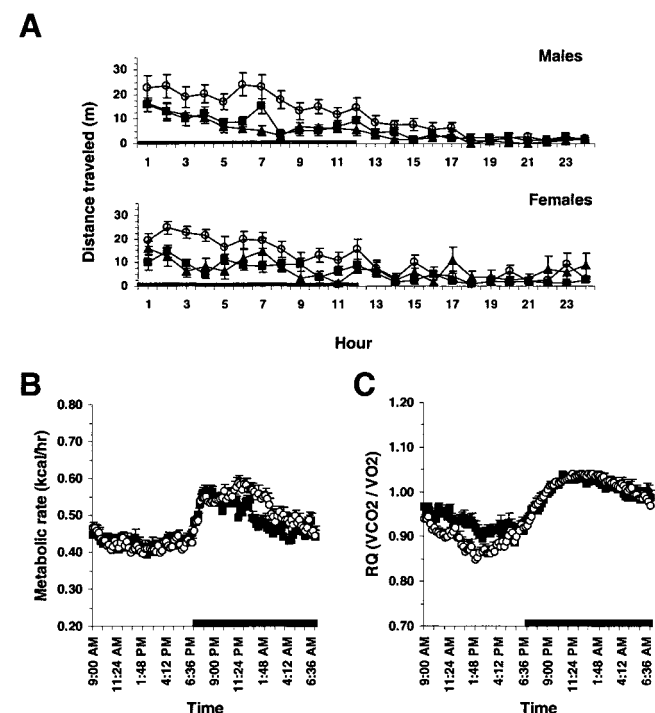

Fig. 3. Appetitive behavior of control and Mch1r⁻/⁻ mice maintained on regular chow. (A) Daily food intake of ≈10-week-old individually housed male wild-type (Mch1r⁺/⁺), Mch1r⁺/⁻, and Mch1r⁻/⁻ (n = 10–11 per genotype), and female Mch1r⁺/⁺ (n = 10), Mch1r⁺/⁻ (n = 4), and Mch1r⁻/⁻ (n = 8) littermates. (B) Daily feeding duration of 8–10-week-old individually housed male Mch1r⁺/⁺ and Mch1r⁻/⁻ littermates (n = 12 per genotype) maintained in a 12-h/12-h light/dark cycle (LD) or constant darkness (DD). White portions of bars represent 12-h light phase (LD) or 12-h subjective day (DD), and shaded portion represents 12-h dark phase (LD) or 12-h subjective night (DD). All P values are from comparisons between Mch1r⁺/⁺ and Mch1r⁻/⁻ littermates. **, $P < 0.001$; *, $P < 0.05$.

light-dark cycle and did not differ when mice were maintained in constant darkness (Fig. 3B), suggesting that the hyperphagia is not a consequence of altered circadian rhythm.

Motor Activity. Mch1r⁻/⁻ mice of both genders, and from both lines, were significantly hyperactive relative to littermate controls when maintained in their home-cages (Fig. 4A), possibly explaining their leanness despite moderate hyperphagia. Mch1r⁻/⁻ mice were twice as active as controls during the dark phase of the light-dark cycle, yet exhibited normal levels of ambulatory activity during the light phase. Mch1r⁻/⁻ mice also exhibited significantly more fine motor movements, as indicated by consecutive breaks of the same photobeam, than controls during the dark phase, but displayed normal levels of fine motor movements during the light phase (data not shown).

Metabolism. Mch1r⁻/⁻ mice exhibited a significantly greater metabolic rate during a portion of the dark phase of the light-dark cycle (Fig. 4B) that was temporally correlated with the period of hyperactivity (data not shown), suggesting that this increase in metabolic rate is secondary to the hyperactivity. The respiratory quotient, an indicator of metabolic fuel preference, was significantly lower in male Mch1r⁻/⁻ mice during the light phase but was indistinguishable from that of wild types during the dark phase (Fig. 4C), implying that Mch1r⁻/⁻ mice rely on the oxidation of free fatty acids and less on glycolysis during periods when they are not actively eating.

Neuroendocrine Function. Plasma glucose, insulin, and triglyceride levels were not significantly different in 5–7-month-old Mch1r⁻/⁻ and wild-type littermates of either gender (Table 1). Plasma leptin and total thyroxine (T4) levels were significantly lower in male Mch1r⁻/⁻ mice relative to wild types, and female levels revealed similar trends (Table 1). Lower leptin levels are consistent with the lean phenotype, and lower T4 levels support the notion that MCH may be involved in the regulation of thyroid function (23). Alternatively, alterations in T4 levels may reflect a compensatory response to the increased energy expenditure.

A

Males

Females

Hour

B

Time

C

Time

A

B

Fig. 5. Response of control and $Mch1r^{-/-}$ mice to DIO. (*A*) Cumulative body weight gains of female wild-type ($Mch1r^{+/+}$) and $Mch1r^{-/-}$ littermates maintained simultaneously on either a regular chow (RC) or a high-fat (HF) diet for 7 weeks ($n = 9–12$ per group). All groups were weight-matched and all mice were 6–8-weeks-old at the initiation of the study. (*B*) Cumulative food intake by mice in *A* during the 7-week period ($n = 9–11$ per group). *P* values are from comparisons between chow and high-fat groups of the same genotype (∗) or between $Mch1r^{+/+}$ and $Mch1r^{-/-}$ littermates maintained on the same diet (∗∗). ∗, $P < 0.05$; ∗∗, $P < 0.001$.

Fig. 4. Energy expenditure of control and $Mch1r^{-/-}$ mice. (*A*) Ambulatory activity of ≈12-week-old individually housed male wild-type ($Mch1r^{+/+}$, $n = 11$; filled squares), $Mch1r^{+/-}$ ($n = 6$; filled triangles), and $Mch1r^{-/-}$ ($n = 11$; open circles), and female $Mch1r^{+/+}$ ($n = 10$), $Mch1r^{+/-}$ ($n = 4$), and $Mch1r^{-/-}$ ($n = 8$) littermates. $Mch1r^{-/-}$ curves were significantly different ($P < 0.005$) from $Mch1r^{+/+}$ and $Mch1r^{+/-}$ curves for the entire dark phase. (*B*) Metabolic rate of ≈8-week-old individually housed male $Mch1r^{+/+}$ ($n = 10$) and $Mch1r^{-/-}$ ($n = 13$) littermates. From 10 p.m. to 5 a.m., the $Mch1r^{-/-}$ curve was significantly different ($P < 0.05$) from the $Mch1r^{+/+}$ curve. (*C*) Respiratory quotient (RQ) of mice from *B*. The $Mch1r^{-/-}$ curve was significantly different ($P < 0.01$) from the $Mch1r^{+/+}$ curve for the entire light phase. Solid horizontal bars represent the dark phases of the studies.

Plasma corticosterone levels were significantly greater in 6–7-month-old male $Mch1r^{-/-}$ mice relative to wild-type littermates (Table 1). This result is consistent with the finding that MCH administration reduces basal and stress-induced plasma adrenocorticotropic hormone levels in rats (24) and suggests that MCH1R may be involved in the regulation of adrenal function.

Neuropeptide Expression. To further investigate the mechanisms underlying the elevated corticosterone levels, we measured corticotrophin-releasing factor (CRF) mRNA in the brain by *in situ* hybridization. CRF mRNA levels in the paraventricular nucleus of the hypothalamus (PVN) were significantly lower in male $Mch1r^{-/-}$ mice relative to wild types, yet were normal in the central nucleus of the amygdala (CEA) (PVN: $Mch1r^{-/-}$, 79.5 ± 9.6 Ci/g of tissue; $Mch1r^{+/+}$, 105.3 ± 10.1 Ci/g tissue; $P < 0.05$; CEA: $Mch1r^{-/-}$, 57.5 ± 1.3 Ci/g of tissue; $Mch1r^{+/+}$, 57.0 ± 5.9 Ci/g of tissue; $n = 5$ per genotype). This finding suggests that the elevated corticosterone levels are not the result of increased hypothalamic CRF. Instead, it is likely that the reduced CRF expression in the PVN is a consequence of negative feedback driven by the elevated levels of corticosterone. In contrast to CRF, hypothalamic levels of NPY, AgRP, galanin, pro-opiomelanocortin, and cocaine- and amphetamine-regulated transcript mRNAs measured during the light phase were all normal in $Mch1r^{-/-}$ mice (data not shown).

Response to Diet-Induced Obesity (DIO). Female wild-type mice maintained on a high-fat diet for 7 weeks gained significantly more body weight than wild-type littermates maintained on regular chow (Fig. 5*A*). In contrast, female $Mch1r^{-/-}$ mice maintained on the high-fat diet gained the same amount of body weight as $Mch1r^{-/-}$ littermates maintained on regular chow. This

Table 1. Neuroendocrine profiles of control and $Mch1r^{-/-}$ mice

	Males		Females	
	$Mch1r^{+/+}$	$Mch1r^{-/-}$	$Mch1r^{+/+}$	$Mch1r^{-/-}$
Leptin, ng/ml	6.05 ± 1.99	2.12 ± 0.08*	3.87 ± 0.92	2.31 ± 0.06
Triglyceride, mg/dl	77 ± 10	69 ± 6	57 ± 7	64 ± 5
Insulin, ng/ml	0.61 ± 0.15	0.57 ± 0.12	0.31 ± 0.04	0.33 ± 0.04
Glucose, mg/dl	140 ± 7	137 ± 5	132 ± 5	123 ± 4
T4, μg/dl	5.35 ± 0.25	4.32 ± 0.23*	4.58 ± 0.37	4.05 ± 0.22
Corticosterone, ng/ml	9 ± 1.1	23.6 ± 5.4*	ND	ND

Plasma leptin, triglyceride, insulin, glucose, and total thyroxine (T4) levels of group-housed male and female 5–7-month-old wild-type ($Mch1r^{+/+}$) and $Mch1r^{-/-}$ littermates from Fig. 2*A* fasted for 4 h prior to blood collection ($n = 10–14$ per group). Plasma corticosterone levels of individually housed 6–7-month-old male wild-type and $Mch1r^{-/-}$ littermates ($n = 9–10$ per genotype) maintained in isolation and fed ad libitum. *, $P \leq 0.05$; ND, not determined.

NEUROBIOLOGY
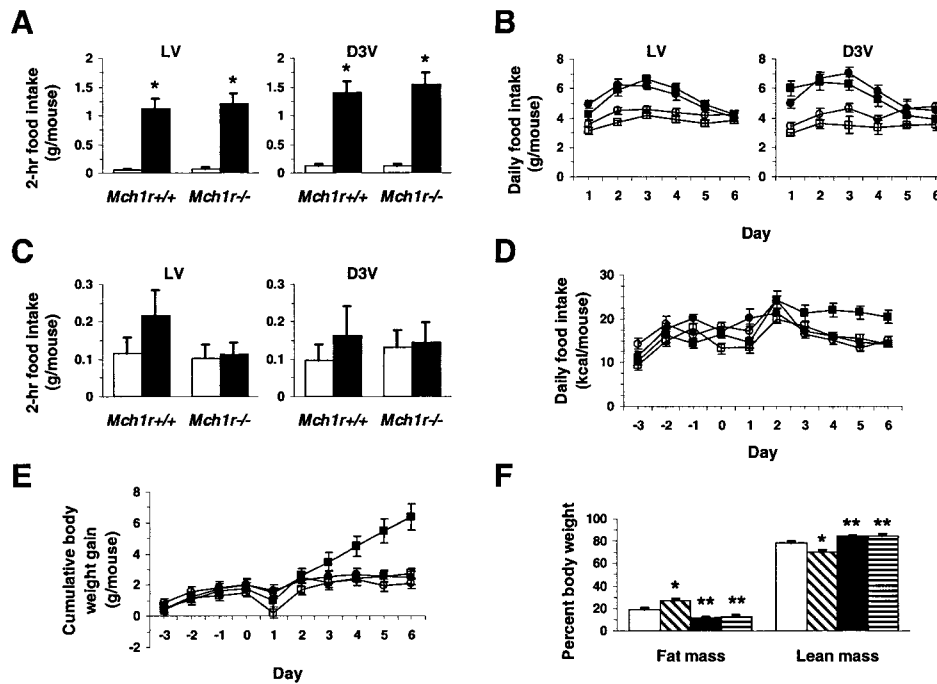
Fig. 6. Response of control and *Mch1r⁻/⁻* mice to intracerebroventricular administration of NPY, AgRP, or MCH. (*A*) Effect of NPY on daytime feeding. NPY (≈0.25 nmol; shaded bars) or vehicle (white bars) were injected into either the left lateral ventricle (LV; *n* = 10–11 per genotype) or the dorsal third ventricle (D3V; *n* = 6–8 per genotype) of 12–14-week-old male wild-type (*Mch1r⁺/⁺*) and *Mch1r⁻/⁻* littermates. Food intake was measured 2 h later. *P* values are from comparisons between treatment groups of the same genotype. *, *P* < 0.001. (*B*) Effect of AgRP on daily feeding. AgRP (≈0.9 nmol; filled symbols) or vehicle (open symbols) were injected into either the LV (*n* = 8–10 per genotype) or the D3V (*n* = 6–10 per genotype) of 18–20-week-old male *Mch1r⁺/⁺* (squares) and *Mch1r⁻/⁻* (circles) littermates on day 0. Food intake was measured daily for 6 days. All AgRP curves were significantly different (LV, *P* < 0.005; D3V, *P* < 0.01) from corresponding vehicle curves. (*C*) Effect of MCH on daytime feeding. MCH (≈2 nmol; shaded bars) or vehicle (white bars) were injected into either the LV (*n* = 9 per genotype) or the D3V (*n* = 5–10 per genotype) of 14–16-week-old male *Mch1r⁺/⁺* and *Mch1r⁻/⁻* littermates. Food intake was measured 2 h later. (*D*) Effect of chronic MCH infusion on daily food intake. Male 11–13-week-old *Mch1r⁺/⁺* (squares) and *Mch1r⁻/⁻* (circles) littermates received chronic D3V infusions of either MCH (≈12 nmol per mouse per day; filled symbols) or vehicle (open symbols) for 6 days (*n* = 9–11 per group). Mice were cannulated and implanted with osmotic pumps containing only vehicle on day −5. On day 0, original pumps were replaced with new pumps containing either vehicle or MCH. Beginning on day 1, all mice were maintained on a moderate fat diet. From days 1 to 6, the *Mch1r⁺/⁺*/MCH treatment curve was significantly different (*P* < 0.005) from the three other curves. (*E*) Effect of chronic MCH infusion on cumulative body weight gain. Body weights of mice from *D* were measured daily, and values from day −4 were used to calculate cumulative body weight gains. From days 1 to 6, the *Mch1r⁺/⁺*/MCH treatment curve was significantly different (*P* < 0.0001) from the three other curves. (*F*) Effect of chronic MHC infusion on body composition. DEXA analysis of body composition was performed on mice from *D* at the end of the 6-day chronic infusion period (*Mch1r⁺/⁺*: vehicle, white bars; MCH, hatched bars; *Mch1r⁻/⁻*: vehicle, shaded bars; MCH, striped bars). *P* values are from comparisons between treatment groups of the same genotype (*) or between genotypes of the same treatment (**). *, *P* < 0.005; **, *P* < 0.01.

decreased susceptibility to DIO is most likely a consequence of the hyperactivity and associated increase in energy expenditure. Interestingly, maintenance on the high-fat diet abolished the significant hyperphagia (24.3%) observed with maintenance on regular chow (Fig. 5*B*). The response of male *Mch1r⁻/⁻* mice to DIO was not evaluated.

Response to Centrally Administered Orexigenics. *Mch1r⁻/⁻* mice exhibited normal responses to both acute left lateral and dorsal third ventricle administrations of NPY (Fig. 6*A*) and AgRP (Fig. 6*B*), demonstrating that MCH1R is not required for their orexigenic actions. Additionally, these data suggest that the hyperphagia is not a consequence of heightened NPY or AgRP signaling. Acute administrations of MCH were without significant effects, but tended to increase the food intake of only wild types (Fig. 6*C*). Subsequently, we evaluated the response of *Mch1r⁻/⁻* and wild-type littermates to chronic dorsal third ventricle infusions of MCH. Six days of chronic MCH treatment resulted in significantly greater food intake (Fig. 6*D*), body weight gains (Fig. 6*E*), and altered body composition (Fig. 6*F*) in wild-types, whereas *Mch1r⁻/⁻* littermates were not affected, demonstrating that MCH1R is required for the orexigenic actions of MCH.

Discussion

Mch1r⁻/⁻ mice are lean, hyperactive, have altered metabolism, are hyperphagic when maintained on regular chow, have an altered neuroendocrine profile, and are less susceptible to DIO. Additionally, *Mch1r⁻/⁻* mice are resistant to the orexigenic actions of MCH, demonstrating that MCH1R is a physiologically relevant MCH receptor. The leanness and decreased susceptibility to DIO are most likely a consequence of the hyperactivity and associated increase in energy expenditure. The hyperphagia on regular chow is surprising in light of previous pharmacological (3, 4) and genetic (8, 9) studies defining MCH as an endogenous orexigen; however, it may be a consequence of the mutants having a greater requirement for nutrients because of their hyperactivity and increased lean mass. Alternatively, this hyperphagia may represent altered nutrient or taste preferences, as the hyperphagia is abolished with maintenance on the high-fat diet. Further studies are required to differentiate between these possibilities.

It is noteworthy that both MCH1R and Pmch deficiencies result in a lean phenotype; however, the mechanisms underlying these phenotypes do not seem to be identical. *Mch1r⁻/⁻* mice are lean because of hyperactivity, whereas *Pmch⁻/⁻* mice are lean because of hypophagia and increased metabolic rate. Other

distinctions include differences in leptin sensitivity (D.J.M., unpublished observation) and neuroendocrine profiles. These distinctions suggest that in addition to MCH deficiency, the absence of other proteins encoded by *Pmch*, such as NEI, neuropeptide GE, MCH-gene-overprinted-polypeptide, or possibly AROM, may contribute to the phenotype of *Pmch*$^{-/-}$ mice. Alternatively, an unidentified MCH receptor subtype may exist in mice and contribute to the phenotypic differences observed between *Pmch*$^{-/-}$ and *Mch1r*$^{-/-}$ mice. It is also possible that MCH1R is capable of ligand-independent signaling, in which case the phenotypes of the ligand and receptor knockouts might differ.

Centrally administered CRF can induce transient increases in locomotor activity (25); however, the chronically elevated glucocorticoid levels seen in patients with Cushing's syndrome (26) or in transgenic mice overexpressing CRF do not result in hyperactivity (27). Thus, it is unlikely that the observed alterations in the hypothalamic–pituitary–adrenal axis underlie the hyperactivity phenotype. Instead, elevated levels of corticosterone could be a consequence of the chronic hyperactivity.

The involvement of the dopaminergic system in the regulation of motor activity is well known. *Mch1r* is expressed in brain regions known to contain dopaminergic cell bodies and projections, for example the striatum and nucleus accumbens (Fig. 1*C*). Consequently, MCH may modulate the dopaminergic system (17). Therefore, it is possible that a dysregulation in dopaminergic signaling might be responsible for the hyperactivity. NEI, another neuropeptide derived from *Pmch* (5), can increase motor activity when administered centrally and these effects can be blocked by prior administration of MCH (28). Consequently, unopposed NEI signaling resulting from MCH1R deficiency could contribute to the hyperactivity. An understanding of the mechanism(s) underlying the hyperactivity phenotype will require further investigation.

We conclude that MCH1R is a physiologically relevant MCH receptor that serves a role in the regulation of energy homeostasis primarily through actions on motor activity but also through effects on metabolism, food intake, and neuroendocrine function. Furthermore, we suggest that other proteins encoded by *Pmch* may also play a role in the regulation of energy homeostasis. These studies validate MCH1R as a potential target for the treatment of human obesity.

1. Nahon, J.-L. (1994) *Crit. Rev. Neurobiol.* **8,** 221–262.
2. Bittencourt, J. C., Presse, F., Arias, C., Peto, C., Vaughan, J., Nahon, J.-L., Vale, W. & Sawchenko, P. E. (1992) *J. Comp. Neurol.* **319,** 218–245.
3. Qu, D., Ludwig, D. S., Gammeltoft, S., Piper, M., Pelleymounter, M. A., Cullen, M. J., Mathes, W. F., Przypek, R., Kanarek, R. & Maratos-Flier, E. (1996) *Nature (London)* **380,** 243–247.
4. Rossi, M., Choi, S. J., O'Shea, D., Miyoshi, T., Ghatei, M. A. & Bloom, S. R. (1997) *Endocrinology* **138,** 351–355.
5. Nahon, J. L., Presse, F., Bittencourt, J. C., Sawchenko, P. E. & Vale, W. (1989) *Endocrinology* **125,** 2056–2065.
6. Toumaniantz, G., Bittencourt, J. C. & Nahon, J.-L. (1996) *Endocrinology* **137,** 4518–4521.
7. Borsu, L., Presse, F. & Nahon, J.-L. (2000) *J. Biol. Chem.* **275,** 40576–40587.
8. Shimada, M., Tritos, N. A., Lowell, B. B., Flier, J. S. & Maratos-Flier, E. (1998) *Nature (London)* **396,** 670–673.
9. Ludwig, D. S., Tritos, N. A., Mastaitis, J. W., Kulkarni, R., Kokkotou, E., Elmquist, J., Lowell, B. Flier, J. S. & Maratos-Flier, E. (2001) *J. Clin. Invest.* **107,** 379–386.
10. Saito, Y., Nothacker, H.-P. & Civelli, O. (2000) *Trends Endocrinol. Met.* **11,** 299–303.
11. Mori, M., Harada, M., Terao, Y., Sugo, T., Watanabe, T., Shimomura, Y., Abe, M., Shintani, Y., Onda, H., Nishimura, O. & Fujino, M. (2001) *Biochem. Biophys. Res. Commun.* **283,** 1013–1018.
12. Hill, J., Duckworth, M., Murdock, P., Rennie, G., Sabido-David, C., Ames, R. S., Szekeres, P., Wilson, S., Bergsma, D. J., Gloger, I. S., *et al.* (2001) *J. Biol. Chem.* **276,** 20125–20129.
13. Sailer, A. W., Sano, H., Zeng, Z., McDonald, T. P., Pan, J., Pong, S. S., Feighner, S. D., Tan, C. P., Fukami, T., Iwaasa, H., *et al.* (2001) *Proc. Natl. Acad. Sci. USA* **98,** 7564–7569.
14. An, S., Cutler, G., Zhao, J. J., Huang, S. G., Tian, H., Li, W., Liang, L., Rich, M., Bakleh, A., Du, J., *et al.* (2001) *Proc. Natl. Acad. Sci. USA* **98,** 7576–7581.
15. Wang, S., Behan, J., O'Neill, K., Weig, B., Fried, S., Laz, T., Bayne, M., Gustafson, E. & Hawes, B. E. (2001) *J. Biol. Chem.* **276,** 34664–34670.
16. Chambers, J., Ames, R. S., Bergsma, D., Muir, A., Fitzgerald, L. R., Hervieu, G., Dytko, G. M., Foley, J. J., Martin, J., Liu, W. S., *et al.* (1999) *Nature (London)* **400,** 261–265.
17. Saito, Y., Nothacker, H.-P., Wang, Z., Lin, S. H. S., Leslie, F. & Civelli, O. (1999) *Nature (London)* **400,** 265–269.
18. Lakaye, B., Minet, A., Zorzi, W. & Grisar, T. (1988) *Biochim. Biophys. Acta* **1401,** 216–220.
19. Papaioannou, V. & Johnson, R. (1993) in *Gene Targeting: A Practical Approach*, eds. Joyner, A. L. (Oxford University, Oxford), pp. 107–136.
20. Sambrook, J., Fritsch, E. F. & Maniatis, T. (1989) in *Molecular Cloning: A Laboratory Manual*, ed. Nolan, C. (Cold Spring Harbor Lab. Press, Plainview, NY), 2nd. Ed., pp. 9.31–9.58.
21. Guan, X. M., Yu, H. & Van der Ploeg, L. H. (1998) *Mol. Brain Res.* **59,** 273–279.
22. Chen, A. S., Metzger, J. M., Trumbauer, M. E., Guan, X. M., Yu, H., Frazier, E. G., Marsh, D. J., Forrest, M. J., Gopal-Truter, S., Fisher, J., *et al.* (2000) *Transgenic Res.* **9,** 145–154.
23. Kennedy, A. R., Todd, J. F., Stanley, S. A., Abbott, C. R., Small, C. J., Ghatei, M. A. & Bloom, S. R. (2001) *Endocrinology* **142,** 3265–3268.
24. Bluet-Pajot, M.-T., Presse, F., Voko, Z., Hoeger, C., Mounier, F., Epelbaum, J. & Nahon, J.-L. (1995) *J. Neuroendocrinol.* **7,** 297–303.
25. Contarino, A., Dellu, F., Koob, G. F., Smith, G. W., Lee, K. F., Vale, W. W. & Gold, L. H. (2000) *Endocrinology* **141,** 2698–2702.
26. Nelson, D. H. (1989) in *Endocrinology*, ed. DeGroot, L. J. (Saunders, Philadelphia), Vol. 2, pp. 1660–1675.
27. Stenzel-Poore, M. P., Heinrichs, S. C., Rivest, S., Koob, G. F. & Vale, W. W. (1994) *J. Neurosci.* **14,** 2579–2584.
28. Sanchez, M., Baker, B. I. & Celis, M. (1997) *Peptides* **18,** 393–396.

NEUROBIOLOGY